

1 **Black crusts on Venetian built heritage, investigation on the impact of pollution sources on their**
2 **composition**

3
4 Mauro F. La Russa^a, Valeria Comite^b, Nevin Aly^c, Donatella Barca^a, Paola Fermo^b, Natalia Rovella^a,
5 Fabrizio Antonelli^d, Elena Tesser^d, Silvestro A. Ruffolo^{e*}
6

7 a Department of Biology, Ecology and Earth Science, Rende, Cosenza, Italy

8 b Department of Chemistry, Università degli Studi di Milano, Milano, Italy

9 c Faculty of Petroleum and Mining Engineering, Suez University, Suez, Egypt

10 d Laboratorio di Analisi dei Materiali Antichi (LAMA), University Iuav di Venezia, Venice, Italy

11 e Department of Molecular Science and Nanosystems, University Ca' Foscari, Venice, Italy

12
13 * Corresponding author: silvestro.ruffolo@unical.it
14

15 **Abstract**

16 This research deals with the characterization of black crusts collected from several historical buildings in
17 the city of Venice. This city suffers from pollution from the industrial area of Marghera, as well as from
18 the maritime traffic. Black crust can be considered as a passive sampler of pollutants, with particular
19 reference to heavy metals. For this reason, in order to fully characterize those samples, several techniques
20 were used, including scanning electron microscopy, thermogravimetric analysis, laser ablation inductively
21 coupled plasma mass spectrometry, infrared spectroscopy and ion chromatography. This integrated
22 approach allowed us to gain information about the mineralogical phases and the elements within the crusts
23 giving the possibility to identify the pollution sources causing the stone decay within the buildings, as well
24 as the variability in composition depending on the exposure of the analyzed surfaces.
25

26 **1. Introduction**

27 Air pollution is one of the most important causes of stone decay in urban environment [1-7]. Among the
28 degradation processes due to airborne pollutants, the formation of black crusts is one of the most dangerous
29 one [1, 8-10]. They are formed thanks to a sulphating processes on the stone surface: calcium carbonate
30 (CaCO₃), which is the main constituent of carbonate rocks, is transformed into gypsum CaSO₄ 2H₂O. The
31 other atmospheric components, such as metals and metal oxides, act as catalysts in the sulphating reaction.
32 This process affects mainly stone materials having carbonate nature (for example limestone, marble,
33 mortar). In addition, during the crust formation, particulate matter, which contains mainly amorphous
34 carbon and several heavy metals, can be embedded into the gypsum, providing then, the characteristic black
35 colour. Currently, emissions from mobile combustion sources (such as cars and boats) are the main agents
36 responsible for pollution, although a significant decrease is expected in Europe within the next decade.
37 Several authors [11-19] showed how the analysis of trace metals into black crust, as well as the
38 characterization of the carbon, can provide insights on the influence of the pollution sources in the formation
39 processes of this degradation product, moreover, they can act as passive samplers of air pollution. In this
40 research, we characterized samples of black crusts collected from several historical buildings in the city of
41 Venice. This city suffers pollution from the industrial area of Marghera, as well as from the maritime traffic.
42 Samples were investigated by means of infrared spectroscopy to detect the main mineralogical phases;
43 electron microscopy coupled with EDS to gain information about the micromorphology and the chemical
44 composition in term of major elements; ion chromatography to investigate the soluble salts within the
45 crusts; thermogravimetric analysis to obtain information on the carbon fraction; ion coupled plasma coupled
46 with laser ablation to characterize the content of trace metals.
47

48
49 **2. Sampling**

50 Eleven samples of black crusts were collected from the city of Venice, from different buildings located in
51 different areas of the island (Fig. 1). For all samples, the stony substrate has been identified as Istria stone,

Eliminato: be

53 a limestones having low porosity, which is quarried in Istria peninsula. Before sampling on each monument,
 54 on-site surveys were carried out in order to identify the most representative points in order to assess
 55 pollution variations across the different areas of the island. Black crust micro-samples and stone substrate
 56 have been taken from several architectural elements (i.e. portals, frames and decorative elements) sheltered
 57 from meteoric water at a height of about 1.50 m, usually from vertical surfaces. There is not any reliable
 58 information about restorations performed in the past on sampled areas. Sampling is summarized in Table 1

59



60

61

Fig. 1. Map of Venice reporting the sampling points

62

63

Sample ID	Description of sampling point
V1	Private building located near Ruga Vecchia, window frame, vertical surface
V2	Next to Canal Grande, portal of a private building, vertical surface
V4	Private building located Rio Megio, portal
V5	Private building next to Rio Megio, decorative architectural element horizontal surface
V6	Via Corte Piossi, church of Santa Maria Mater Domini, lower part, vertical surface
V7	Piazza San Marco, vertical surface
V8	Piazza San Marco, inner part of the colonnade, vertical surface
V9	Campo San Maurizio, left side of private building next to Museo della Musica, vertical surface
V10	Next to Rio di San Pantalon left side of a portal belonging to a private building, vertical surface
V11	Next to Museo Guggenheim (Canal Grande), wall of private building, vertical surface
V12	Next to the church of St. Moisè, inner part of a portal, private building, vertical surface

64

Table 1. Summary of collected samples

65 3. Analytical methods

66 Fourier-transform infrared spectroscopy (FT-IR) investigations were carried out to identify the
67 mineralogical phases constituting the examined damage layers. The infrared spectra were collected with a
68 spectrophotometer Nicolet 380 (Thermo Electron Corporation) equipped with attenuated total reflection
69 (ATR) accessory Smart Orbit and interfaced with a microscope FT-IR Nicolet Centaurus. The ATR
70 accessory is equipped with a crystal diamond while on the microscope it is possible to mount an accessory
71 with a silicon crystal (μ ATR), in the range 500–4000 cm^{-1} at a resolution of 4 cm^{-1} . The technique was
72 used to analyse small amounts of black crust drawn from samples surfaces using a scalpel.

73 In order to observe the micro-morphology, analyse the major elements and map the distribution of elements
74 on a microscopic scale, an Electron Probe Micro Analyzer (EPMA) - JEOL- JXA 8230 – coupled with a
75 spectrometer EDS – JEOL EX-94310FaL1Q - Silicon drift type - has been used. Elemental maps have been
76 acquired with the following parameters: HV- 15 keV; Probe current - 10 nA; Working Distance - 11mm;
77 Take off - 40°; Live Time - 50 sec.

78 Ion Chromatography (IC) has been employed for the quantification of the main ions. Three milligrams of
79 powder, withdrawn from the sample surface, have been placed in a test tube and treated with 3 mL of MilliQ
80 water. The test tubes have been put in an ultrasonic bath for 1 h, then the solutions centrifuged and injected
81 for IC analyses by means of an auto-sampler. Measurements of cationic (Na^+ , K^+ , Ca^{2+} , Mg^{2+} and NH_4^+)
82 and anionic (NO_2^- , NO_3^- , SO_4^{2-} , Cl^-) species were carried out by using an ICS-1000 HPLC system equipped
83 with a conductivity system detector. Anions analysis was carried out with an Ion Pac AS14A column using
84 8 mM Na_2CO_3 /1 mM NaHCO_3 , flow rate = 1 mL/min with for the detection a conductivity system detector
85 working with an anion self-regenerating suppressor ULTRA (ASRS-ULTRA) suppression mode. Cations
86 determination was performed using a CS12A (Dionex) column and 20 mM methane sulfonic acid (MSA)
87 as eluent at a flow rate=1 mL/min and for the detection a conductivity system equipped with a cation self-
88 regenerating suppressor-ULTRA (CSRS-ULTRA) suppression mode.

89 Thermogravimetric analyses (TG) were carried out on a selected group of samples by a Mettler Toledo
90 TGA/DSC 3+ instrument, which allows simultaneous TG and DSC analyses. The analyses were conducted
91 in the range 30°- 800° C, increasing the temperature with a rate of 20° C/minute, using about 0.2 mg of
92 sample for each analysis. The samples were analyzed in the inert and oxidizing atmosphere, the latter made
93 it possible to calculate the EC value.

94 Chemical analyses of the black crusts, as well as of the substrates, in terms of trace elements were performed
95 by laser ablation-inductively coupled plasma-mass spectrometry (LA-ICP-MS). This method can
96 investigate a great number of elements with spot resolutions of approximately about 40–50 μm , which also
97 allows the determination of micrometric compositional variations [20-22]. Analyses were carried out using
98 an Elan DRCe instrument (Perkin Elmer/SCIEX), connected to a New Wave UP213 solid-state Nd-YAG
99 laser probe (213 nm). Samples were ablated by a laser beam in a cell following the method tested by [23].
100 The ablation was performed with spots of 40–50 μm with a constant laser repetition rate of 10 Hz and
101 fluence of $\sim 20 \text{ J/cm}^2$. Calibration was performed using the NIST 612-50 ppm glass reference material as
102 the external standard [24]. Internal standardization to correct instrumental instability and drift was achieved
103 using CaO concentrations from SEM-EDS analyses [25]. The accuracy was evaluated on BCR 2G glass
104 reference material and on an in-house pressed-powder cylinder of the standard Argillaceous Limestone
105 SRM1d of NIST [13]. The resulting element concentrations were compared with reference values from the
106 literature [26]. The accuracy, as the relative difference from reference values, was always better than 12 %,
107 and most elements plotted in the range of $\pm 8 \%$. Analyses were performed both on the black crust and on
108 the unaltered substrate with the aim of better investigating the geochemical variability.

109 4. Result and Discussion

110

111

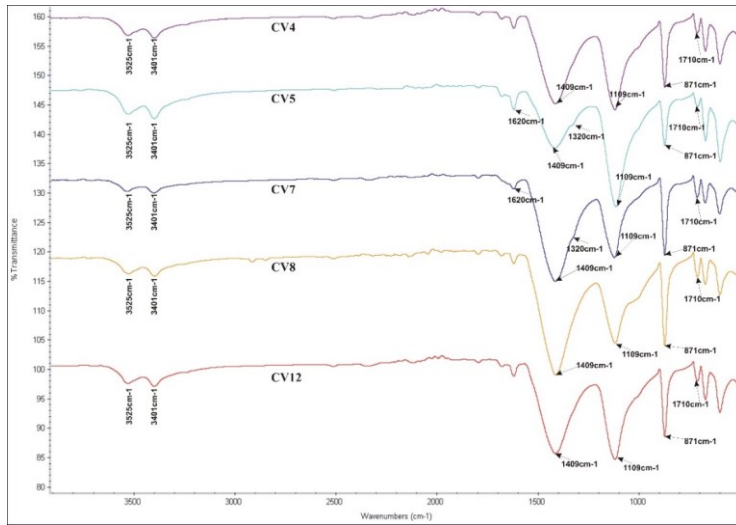


Fig 2. FTIR spectra of crust samples V4, V5, V7, V8 and V12

112
113
114
115
116
117
118
119
120
121
122
123
124

FTIR analysis showed the main inorganic components of the investigated samples. Spectra (Fig.2) shows the characteristic absorption peaks of gypsum, centered at 3525, 3401, 1682, 1627, 1109, 667 and 596 cm^{-1} , as well as the stretching and bending vibrations of the calcium carbonate, with peaks at 1409, 871 and 710 cm^{-1} can be certainly ascribable to the underlying substrate. The presence of oxalate (with peaks at 1630, 1320 and 780 cm^{-1}) in samples V5 and V7, according to the literature could be attributed due to restoration works carried out in the past or to the activity of microorganism colonies [26-33].

Electron microscopy coupled with EDS was performed in order to acquire information micromorphological (Fig. 3) and chemical (in terms of major elements) features of crusts. The microanalysis was carried out on spots of each sample.

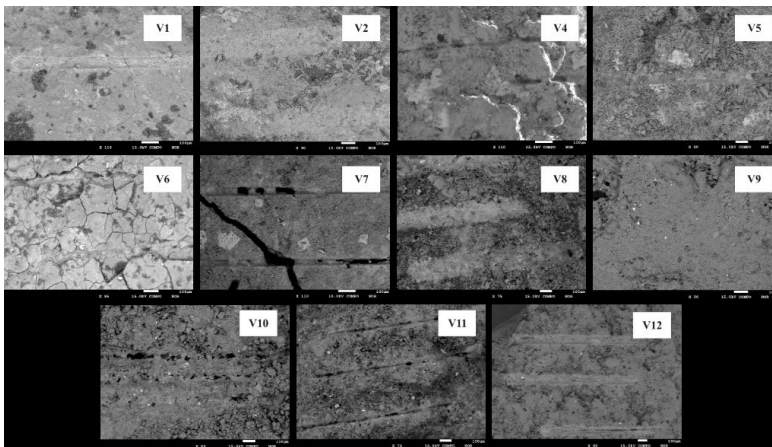


Fig. 3. Electron microscope images of samples

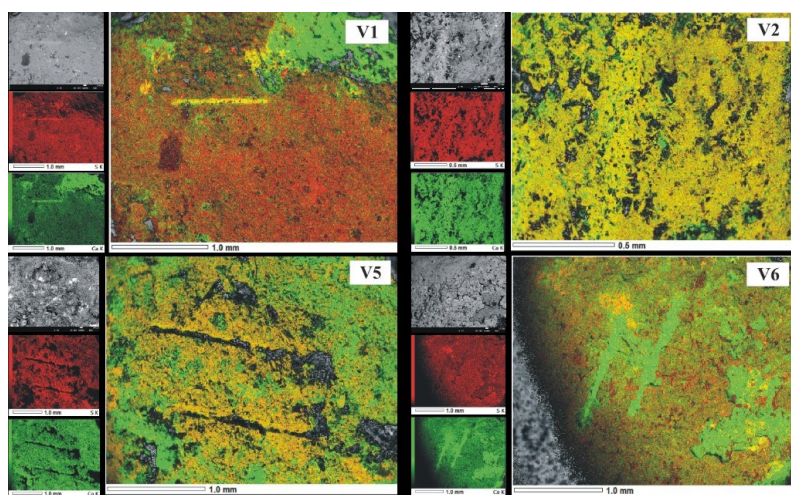
125
126

127
 128 The analyzed crusts show in most cases, a heterogeneous, dendritic and irregular morphology (V2, V4, V5,
 129 V8, V9, V10, V11 and V12), while, few samples show a linear and compact morphology (V1, V6 and V7).
 130 The black crusts analyzed consist of gypsum crystals with acicular and lamellar habitus. Particles from
 131 combustion, having a spherical and sub-spherical shape with a smooth or porous surface were identified;
 132 they are heterogeneously distributed along the whole examined surface.
 133 In general, the crusts examined show the same chemical composition with high levels of S and Ca, followed
 134 by Si, Al, Fe, Na, and smaller amounts of K, Mg and P (Table 2)
 135

Sample	Na (% wt)	Mg (% wt)	Al (% wt)	Si (% wt)	P (% wt)	S (% wt)	Cl (% wt)	K (% wt)	Ca (% wt)	Fe (% wt)
V1	1.3	1.8	9.6	4.8	0.9	34.2	1.7	1.9	31.8	9.4
V2	1.3	0.8	2.7	11.8	0.6	42.1	1.3	0.9	33.2	5.0
V4	1.3	1.1	6.7	5.6	0.5	42.8	1.7	0.8	36.3	1.0
V5	1.1	1.3	2.8	9.8	0.0	40.4	1.6	1.0	40.1	1.6
V6	1.2	2.0	11.0	4.0	0.0	36.9	1.5	1.8	35.0	5.2
V7	1.1	1.1	2.4	4.7	1.7	40.5	5.8	1.3	41.1	0.0
V8	1.3	1.5	2.7	7.7	1.0	44.1	2.2	0.0	39.1	0.0
V9	1.3	1.0	3.3	8.5	0.5	45.7	1.0	1.8	34.0	2.5
V10	1.8	2.0	3.4	4.1	0.5	37.3	7.9	2.6	35.0	2.4
V11	1.4	2.1	6.3	7.0	1.0	37.2	3.2	2.8	33.4	4.7
V12	1.1	1.1	2.3	6.8	1.5	42.5	2.6	0.0	36.8	5.0

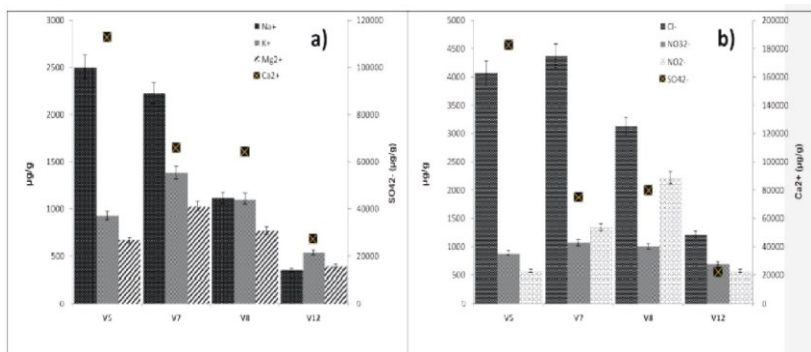
136 **Table 2.** Concentrations of major elements on black crust surfaces measured by EDS
 137
 138
 139

140 In order to evaluate the distribution of the most abundant elements detected in the window analyzed (S and
 141 Ca), it has been performed false color maps of the two elements, as well as a combination of them (Fig 4).
 142



143 **Fig. 4.** EDS Elemental distribution maps
 144

145
 146 The analyses were performed on all samples, some of them are reported in Fig. 4 (V1, V2, V5 and V6).
 147 It is observed that the surface analyzed is mainly composed of gypsum, given by sulfur and calcium whose
 148 content varies from orange to yellow (overlapping of red colors indicating 100% of S and green indicating
 149 100% of Ca) according to the greater or lesser quantity of them.
 150 The samples showing a linear and compact surface (V1 and V6) have a higher sulfur content with a more
 151 homogeneous composition compared to those samples having dendritic irregular morphology (V2 and V5)
 152 which exhibits a heterogeneous gypsum distribution.
 153 Results regarding the determination of ionic species measured by IC are reported in Fig. 5. As expected,
 154 the examined crusts contain large quantities of sulphate, coming from calcium sulphate [33-35]. It is worth
 155 noting that calcium and sulphate show exactly the same trend confirming the presence of gypsum. Among
 156 anions it is quite interesting the presence of high concentrations of nitrites (higher than nitrates for samples
 157 V7, V8 and V9). In the aerosol, particulate matter nitrites are not generally present in concentrations
 158 comparable to nitrates because of the oxidizing conditions so we can hypothesize that they form on the
 159 surface and perhaps can acts as oxidizing agents. Among cations the presence of ammonium is highlighted
 160 only in one case (sample V5), probably due to ammonium salts present in the aerosol PM reacted with the
 161 surfaces transforming into other species.
 162



163
 164 **Fig. 5.** Anions and Cations concentrations (µg/g) of the representative black crusts samples V4, V5, V7,
 165 V8 and V12
 166

167 In Fig. 6 it is shown the apportionment between sea salt sulphate (SS_SO4) and the non-sea salt sulphate
 168 (NSS_SO4) in accordance with what proposed by Keene et al. [36] and Hawley et al. [37], and based on
 169 the mass concentrations of the reference ionic species using the following algorithm: $[NSS_SO4] = [SO4]$
 170 $- (0.25 * [Na])$. As expected sulphate is mainly due to other sources different from sea salt whose
 171 contribution is negligible. Nevertheless, it is worth noting that in a recent study carried out on particulate
 172 matter (PM10) sources due to ship contribution [38] approximately 60% of the total sulphate was attributed
 173 to secondary sources and around 20% was attributed to heavy oil combustion. As a consequence ships
 174 combustion emissions are an important sulphate source contributing to crusts formation.
 175

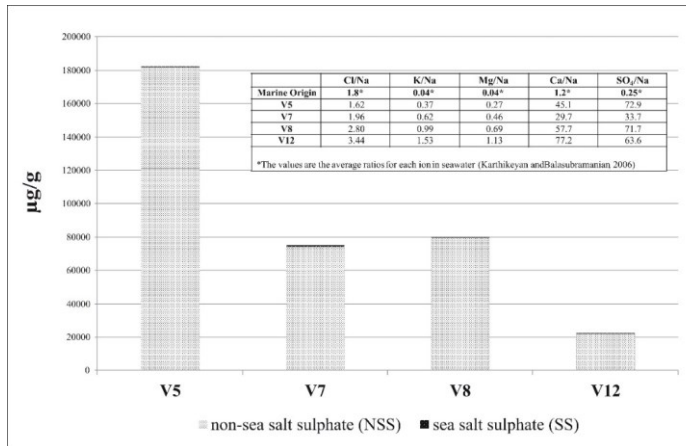


Fig. 6. Histograms showing the sulfate concentrations subdivided in sea salt sulfate (SS_SO4) and the non-sea salt sulfate (NSS_SO4), the representative black crusts samples V5, V7, V8 and V12.

In order to determine the contribution of marine source to crusts composition, in accordance with what proposed by Karthikeyan and Balasubramanian [39], some ratios were calculated taking Na as reference element. In the inset of Fig. 6, the ratios (i.e. Cl/Na, K/Na, Mg/Na, Ca/Na and SO₄²⁻/Na) typical for seawater are reported as a comparison together with the same ratios calculated for the four examined samples. Only Cl/Na ratios are in accordance with what observed in seawater confirming the presence of sodium chloride. Obviously, for Ca²⁺ and sulphate the ratios are significantly different, since Ca is among the main constituents of the crust and sulphate, as mentioned before, has secondary origin. In addition, potassium is linked to other sources such as biomass burning [40-42].

Sample	OC _{TGA} %	CC _{TGA} %	EC _{TGA} %	OC/EC	EC/TC
V4	0.32	7.80	0.47	0.68	0.59
V5	0.41	5.11	0.32	1.28	0.44
V7	0.63	8.33	0.16	3.94	0.20
V8	0.99	7.60	0.82	1.21	0.45
V12	0.26	10.3	0.59	0.44	0.70

Table 3. TC (Total Carbon), OC (Organic Carbon), EC (Elemental Carbon) and CC (Carbonate Carbon) concentrations (wt%) determined for the five black crusts (V4, V5, V7, V8 AND V12) using the TGA methodology.

The quantification of TC (Total carbon), OC (Organic Carbon), EC (Elemental Carbon) and CC (Carbonatic Carbon) in the black crusts (Table 3) has been carried out using a new methodology based on TGA analysis and described in details in another paper in preparation. In particular, OC, EC and CC concentration have been determined taking into account the characteristic weight loss ranges typical of these species (range from 0.26 to 0.99 for OC; from 0.16 to 0.82 for EC and from 5.11 to 10.3 for CC). This methodology has been applied because it is not possible to quantify these species with this analytical method, Thermal Optical Transmittance normally used for this purpose [35]. Thermal Optical Transmittance cannot be applied to the analysis of powder samples since this method requires that the

powder is homogeneously dispersed on a quartz fiber filter. In fact, this technique has been developed for the analysis of organic and elemental carbon in the aerosol particulate matter that is directly sampled on this kind of filters.

EC/TC ratios range from 0.2 to 0.70 and indicate an important contribution of fossil fuel combustion processes, likely due to primary emissions of the intense maritime traffic in the Venice lagoon [43].

Chemical characterization of samples in terms of trace elements was performed using LA-ICP-MS methodology. Three measurements were performed on the crust and on the substrate. The average concentrations (in ppm) of the most representative chemical elements reported in Table 4.

Commentato [v1]: Testo aggiunto

Formattato: Tipo di carattere: (Predefinito) Times New Roman, 11 pt, Colore carattere: Rosso, Inglese (Regno Unito), Non Evidenziato

Black Crust	Concentration (ppm)											
	As	Ba	Cd	Cr	Cu	Ni	Pb	Sb	Sn	Ti	V	Zn
V1	191.9	543.0	5.5	64.6	54.5	25.9	4105.6	15.4	71.0	1231.1	126.4	372.2
V2	93.1	1523.9	33.2	95.7	150.1	57.9	2468.6	28.6	30.2	2209.7	327.8	16996.8
V4	54.2	166.4	2.0	29.1	28.6	13.4	105.0	4.3	15.8	752.8	26.3	370.7
V5	56.2	568.7	3.3	59.5	62.7	22.9	658.5	7.5	29.6	730.0	64.0	626.1
V6	141.1	526.6	11.6	87.7	93.7	24.2	256.9	15.7	12.4	733.3	77.9	350.1
V7	431.9	564.7	5.0	66.9	145.1	355.4	18.3	64.5	943.9	4.5	137.7	169.2
V8	155.8	537.7	3.1	75.9	954.4	211.5	8.5	35.1	966.1	3.8	50.2	325.3
V9	286.5	1240.4	5.7	33.7	66.4	514.5	10.0	70.6	509.6	3.2	41.9	150.2
V10	75.1	2505.1	11.1	79.8	80.7	177.4	7.5	127.7	3082.6	3.0	58.7	716.2
V11	263.1	690.6	4.1	68.9	56.9	71.7	9.9	36.9	645.4	2.4	140.2	126.2
V12	123.3	331.2	4.0	55.4	76.2	504.6	12.6	41.4	336.9	11.4	33.1	126.9
Substrate	Concentration (ppm)											
	As	Ba	Cd	Cr	Cu	Ni	Pb	Sb	Sn	Ti	V	Zn
V1	215.4	75.0	46.9	41.0	344.3	83.2	11291.2	20.1	591.4	2778.7	70.1	2190.0
V2	10.4	105.9	25.1	13.4	65.8	12.1	76.8	6.0	4.7	1735.0	53.5	3546.3
V4	5.7	78.2	0.6	5.0	12.3	4.9	44.6	0.5	20.6	88.1	11.1	162.6
V5	38.5	50.7	0.6	13.8	11.5	4.5	40.6	0.4	11.9	149.9	7.1	99.0
V6	8.6	82.6	1.8	14.0	20.2	12.8	50.6	10.5	3.2	507.6	19.3	56.1
V7	53.7	159.8	1.3	13.7	38.8	45.0	1.0	7.4	127.9	1.2	14.0	43.8
V8	58.8	453.9	1.3	30.1	271.6	311.5	3.9	17.1	570.1	3.8	72.7	260.6
V9	35.7	177.7	0.7	10.0	83.2	66.8	1.7	6.1	815.5	3.4	19.0	104.5
V10	74.6	1471.2	6.2	111.0	279.0	935.2	9.6	31.9	1805.0	7.1	111.5	10915.7
V11	13.7	317.4	1.5	10.0	39.0	25.9	1.2	7.8	411.0	0.4	11.8	63.5
V12	31.8	69.6	2.6	37.6	92.4	493.2	2.8	13.4	364.4	6.4	44.6	475.0

Table 4. Average concentration (ppm) of metals in black crusts and unaltered substrates of samples measured by LA-ICP/MS.

In general, the crusts show higher concentrations of trace metals in comparison with unaltered substrate for almost all metals, such as As, Ba, Cd, Cu, Ni, Pb, Sb, Sn, V and Zn. Some relevant ranges of concentrations are: As (max: 263 in V11 and min: 41.1 in V6), Ba (max: 1523 in V2 min: 116 in V4), Cd (max: 11.6 in V6 and min: 1.97 in V4), Cr (max: 95.7 in V2 and min: 29.1 in V4), Cu (max: 150 in V2 and min: 28.6 in V4), Ni (max: 355 in V7 and min: 13.4 in V4), Pb (max: 2469 in V2 and min: 7.50 in V10), Sb (max: 128 in V10 and min: 4.30 in V4), V (max: 328 in V2 and min: 26.3 in V4) Zn (max: 16997 in V2 and min: 126 in V11). In substrates: As (max: 215 in V1 and min: 5.17 in V4), Ba (max: 1471 in V10 min: 50.7 in V5),

221 Cd (max: 46.9 in V1 and min: 0.55 in V5), Cr (max: 41.0 in V1 and min: 5.04 in V4), Cu (max: 344 in V1
 222 and min: 12.3 in V4), Ni (max: 935 in (Max: 31.9 in V11 and min: 0.54 in V4), V (max: 70.1 in V1 and
 223 min: 11.1 and min: 5.54 in V5), Pb (max: 11291 in V1 and min: 1.16 in V11), Sb in V4), Zn (max: 10916
 224 in V10 and min: 43.8 in V7). In order to better understanding the enrichments of the analyzed metals in
 225 black crust compared with the stony substrate, it has been calculated the enrichment factors as the ratios of
 226 crust/substrate metals' concentration. Results are reported in Table 6.
 227

Element	Enrichment factor EF											
	As	Ba	Cd	Cr	Cu	Ni	Pb	Sb	Sn	Ti	V	Zn
V1	0.9	7.2	0.1	1.6	0.2	0.3	0.4	0.8	0.1	0.4	1.8	0.2
V2	9.0	14.4	1.3	7.1	2.3	4.8	32.2	4.7	6.4	1.3	6.1	4.8
V4	9.5	2.1	3.1	5.8	2.3	2.7	2.4	8.4	0.8	8.5	2.4	2.3
V5	1.5	11.2	5.9	4.3	5.5	5.0	16.2	21.1	2.5	4.9	9.0	6.3
V6	16.3	6.4	6.5	6.3	4.6	1.9	5.1	1.5	3.9	1.4	4.0	6.2
V7	8.0	3.5	3.8	4.9	3.7	7.9	19.2	8.8	7.4	3.7	9.8	3.9
V8	2.6	1.2	2.3	2.5	3.5	0.7	2.2	2.0	1.7	1.0	0.7	1.2
V9	8.0	7.0	8.3	3.4	0.8	7.7	5.8	11.7	0.6	1.0	2.2	1.4
V10	1.0	1.7	1.8	0.7	0.3	0.2	0.8	4.0	1.7	0.4	0.5	0.1
V11	19.2	2.2	2.7	6.9	1.5	2.8	8.5	4.7	1.6	6.4	11.9	2.0
V12	3.9	4.8	1.6	1.5	0.8	1.0	4.4	3.1	0.9	1.8	0.7	0.3

228 **Table 6.** Enrichment factors (EF) of trace metals in black crusts with respect to the substrates
 229
 230

231 Samples show an enrichment ranging from moderate (EF from 3 to 8 in most samples) to high (EF up to
 232 32 for Pb and 14 for Ba in sample V2).

233 The different EF values in the 11 samples can be due to several factors, such as: sampling height, different
 234 morphology of sampled surfaces (vertical or horizontal), different exposure to agents pollutants,
 235 atmospheres, wash out and marine aerosols.

236 In general, the enrichment observed is mainly due to mobile emission sources, since the samples have been
 237 collected at a height of about 1.50 m. The stone substrate at this height is significantly influenced by the
 238 exhaust emitted by the maritime transport vessels (motorboats and boats) that cross the Grand Canal and
 239 the roads, which by spraying and deposition of marine aerosols. In fact, the marine water in Venice is
 240 enriched in metals, mainly Zn, Pb and Cu.

241 Specifically, the highest values were achieved for the V2 sample taken on the Grand Canal in a heavy traffic
 242 area. V5 sample shows high enrichment both for its position near to the Grand Canal, and because it was
 243 sampled from a horizontal decorative surface, where the deposition of the pollutants is higher. V1 and V10
 244 samples show the lowest concentrations (with EF values even below 1), because they come faraway from
 245 direct emission sources.

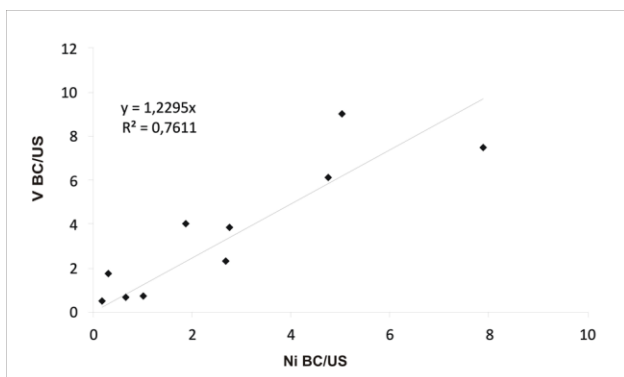
246 Specifically, the high concentrations of Pb, and Zn, observed, are in agreement with the use of leaded gas
 247 [44], used up to a few decades ago. In addition, heavy metals such as Ba, Cu, Ni, Cr and V can be attributed
 248 to the use of other fuels such as fuel oil, diesel and gasoline [44-46], widespread after the abolition of leaded
 249 gasoline.

250 Moreover, it has to be taken into account the contribution of the various industries (such as glassworks, oil
 251 refineries and metallurgy production) located between Porto Marghera and Mestre [47-49], which emit
 252 large amounts quantities of: As, Cd, Sb, Pb, Zn, Cu, Sn, Ni, Cr and V [50-52].

253 In Fig. 7, it has been shown the good correlation between enrichment factors for V and Ni respectively.
 254 These two elements are the typical markers for fossil fuel combustion [38, 43]. In particular, V and Ni can

255 be used as valid tracers of shipping emissions confirming again the role of maritime traffic in the lagoon in
256 the black crusts formation.

257



258

259 **Fig 7.** Correlation between the enrichment factors for V and Ni in the examined samples.

260

261

262 **Conclusions**

263 Black crusts, which are formed on stone materials, have been collected from several historical buildings in
264 the city of Venice and analysed by several analytical techniques. This city suffers pollution from the
265 industrial area of Marghera, as well as from the maritime traffic. Results indicated that the crusts are mainly
266 composed by gypsum with lower content of calcite and oxalates. In terms of major elements, beside calcium
267 and sulphur, Si, Al, Fe, Na, and smaller amounts of K and Mg were identified. Sulphates are mostly
268 ascribable to fuel and biomass combustion, rather than to sea spray, while carbon into the crusts coming
269 from fossil fuel combustion. Regarding trace metals in all samples, As, Ba, Pb and Zn are the most
270 abundant, moreover, the correlation between Ni and V content measured in black crusts, suggests that heavy
271 oil combustion from ship traffic, represent a significant pollution source. It has been observed different
272 pattern of metal concentrations within the crusts in function of the exposure of the sampled surfaces. In
273 particular, those surfaces next to the canals are more enriched in heavy metals, especially Pb, As and Sb,
274 this suggest that also the sea spray can play also a significant role in the deposition of such metals on the
275 stone surface.

276

277

278 **Acknowledgments**

279 This research was supported by Executive Programme for scientific and technological cooperation between
280 the Italian and the Arab Republic of Egypt 2016-2018, project "Characterization of black crusts formed on
281 historic buildings under different levels of ambient air pollution in Cairo and Venice".

282

283 **REFERENCE**

284 [1] G.G. Amoroso, V. Fassina, *Stone Decay and Conservation* (Elsevier, Amsterdam, 1983), 11, 453.

285 [2] A Bonazza et al., *Pollut. Atmos. Numéro Spéc. 7* (2007)

286 [3] P. Brimblecombe, *Urban Air Pollution—European Aspects*, edited by J. Finger, O. Herter, F. Palmer,
287 7 (Kluwer, Dordrecht, 1999)

- 288 [4] P. Brimblecombe, *J. Archit. Conserv.* 6, 30 (2000)
- 289 [5] M. Del Monte, C. Sabbioni, O. Vittori, *Atmos. Environ.* 15, 645 (1981)
- 290 [6] A.V. Turkington, B.J. Smith, W.B. Whalley, *Proceedings of the 4th Int. Symp. Conservation of*
291 *Monuments in the Mediterranean Basin*, Rhodes, 1997, edited by Technical Chamber of Greece, 359
- 292 [7] G. Zappia, *et al.*, *Sci. Total Environ.* 224, 235 (1998)
- 293 [8] A. Moropoulou, A. Cakmak, G. Biscontin, *Materials Research Society Publishing, V. (Crushed*
294 *brick/limemortars of Justinian's, Pittsburgh, 1997)*
- 295 [9] S.J. Antill, H.A. Viles, *Aspects of stone weathering, decay and conservation* (Imperial College Press;
296 London, 1999)
- 297 [10] B.J. Smith, *et al.*, *Environ.* 38, 1173 (2003)
- 298 [11] P. Maravelaki-Kalaitzaki, *et al.*, *Acta*, Part B 52, 41 (1997)
- 299 [12] P. Maravelaki-Kalaitzaki, G. Biscontin, *Atmos. Environ.* 33, 1699 (1999)
- 300 [13] D. Barca, *et al.*, *Environ. Sci. Pollut. Res.* 17, 1433 (2010)
- 301 [14] D. Barca *et al.*, *J. Anal. At. Spectrom.* 26, 1000 (2011)
- 302 [15] D. Barca *et al.*, *Appl. Geochem.* 48, 122 (2014)
- 303 [16] V. Comite, *et al.*, *Rendiconti Online della Società Geologica Italiana*, Arcavacata di Rende 2012
304 edited by S. Critelli, F. Muto, F. Perri, F.M. Petti, M. Sonnino, A. Zuccari. Vol. 21(86° Congr. Naz. Società
305 Geologica Italiana Roma, 2012)
- 306 [17] C.M. Belfiore *et al.*, *Environ. Sci. Pollut. Res.* 20, 8848 (2013).
- 307 [18] M.F. La Russa *et al.*, *Appl. Phys. A Mater. Sci. Process.* 113, 1151(2013)
- 308 [19] S.A. Ruffolo *et al.*, *Sci. Total Environ.* 502, 157 (2015)
- 309 [20] B. Gratuze, *J. Archaeol. Sci.* 26:869 (1999)
- 310 [21] E. Vander Putten, *et al.*, *Anal. Chim. Acta*; 378, 261 (1999)
- 311 [22] T. Wyndham, *et al.*, *Geochim. Cosmochim. Acta*; 68, 2067 (2004)
- 312 [23] D. Gunther, C.A. Heinrich, *J. Anal. At. Spectrom.* 14, 1363(1999)
- 313 [24] N.J.G. Pearce, *et al.*, *Geostand. Newsl.*, 1(21), 115 (1997)
- 314 [25] B.J. Fryer, S.E. Jackson, H.P. Longrich, *Can. Mineral.* 33, 303(1995)
- 315 [26] S. Gao, *et al.*, *Geostand. Newsl.* 26, 181 (2002)
- 316 [27] M. Del Monte, C. Sabbioni, *Environ. Sci. Technol.* 17, 518 (1983)
- 317 [28] C. Sabbioni, G. Zappia, *Aerobiologia* 7, 31 (1991)
- 318 [29] M. Monte, *J. Cult. Herit.* 4, 255 (2003)
- 319 [30] G. Barone *et al.*, *Environ. Geol.* 55, 449 (2008)
- 320 [31] A. Lluveras *et al.*, *Appl. Phys. A* 90, 23 (2008)
- 321 [32] C.M. Belfiore *et al.*, *Appl. Phys. A* 100, 835 (2010)
- 322 [33] D. Gulotta, *et al.*, *Earth Sci.* 69(4), 1085 (2013)]
- 323 [34] P. Fermo *et al.*, *Environ. Sci. Pollut. Res.* 22 (8), 6262 (2015)

- 324 [35] M.F. La Russa *et al.*, *Sci Tot Environ* 593–594, 297 (2017)
- 325 [36] W.C. Keene *et al.*, *J. Geophys. Res.* 91 (D6), 6647 (1986)
- 326 [37] A.M.E. Hawley, J.N. Galloway, W.C. Keene, *Water Air Soil Pollut.* 42, 87 (1988)
- 327 [38] M.C. Bove *et al.*, *Atmos. Environ.*, 125, 140 (2016)
- 328 [39] S. Karthikeyan, R. Balasubramanian, *Microchem. J.*, 82 (1), 49 (2006)
- 329 [40] A. Caseiro, *et al.*, *Atmos. Environ.*, 43, 2186 (2009)
- 330 [41] A. Piazzalunga, *et al.*, *Anal Bioanal Chem.*, 405, 1123 (2013)
- 331 [42] A. Piazzalunga, *et al.*, *Int. J. Environ. Anal. Chem.*, 90, 934 (2010)
- 332 [43] E. Gregoris, *et al.*, *Environ Sci Pollut Res* 23, 6951(2016)
- 333 [44] C. Rodriguez-Navarro, E. Sebastian, *Sci. Total Environ.* 187, 79(1996)
- 334 [45] D. Contini, *et al.*, *J Environ Management* 92:2119 (2011)
- 335 [46] M.D. Geller, *et al.*, *Atmos Environ* 40, 6988(2006)
- 336 [47] B. Pavoni, *et al.*, *Changes in an estuarine ecosystem. The Lagoon of Venice as a case study.* (The
337 Science Society of Global Change. American Chemical Society, Washington, DC, 1992)
- 338 [48] L.G. Bellucci, *et al.*, *Sci Total Environ* 295, 35 (2002)
- 339 [49] R. Zonta, *et al.*, *Mar Pollut Bull* 55, 529(2007)
- 340 [50] M.D. Geller, *et al.*, *Atmos. Environ.* 40, 6988 (2006)
- 341 [51] H. Harmens, *et al.*, *Atmos. Environ.* 41(31), 6673 (2007)
- 342 [52] H. Harmens, D.A. Norris, *The Participants of the Moss Survey, Spatial and Temporal Trends in Heavy*
343 *Metal Accumulation in Mosses in Europe (1990–2005)*, ICP Vegetation Programme, Coordination Centre,
344 Centre for Ecology & Hydrology/Natural Environment Research Council (2008)